J Nanopart Res (2014) 16:2561
DOI 10.1007/s11051-014-2561-5

RESEARCH PAPER

Synthesis and application of non-agglomerated ITO nanocrystals via pyrolysis of indium–tin stearate without using additional organic solvents

Shaojuan Luo · Dongning Yang · Jiyun Feng · Ka Ming Ng

Received: 28 May 2014 / Accepted: 8 July 2014 / Published online: 25 July 2014

Abstract Indium–tin stearate precursor was successfully synthesized by a direct reaction between metals (indium and tin) and molten stearic acid under a nitrogen atmosphere at 260 °C for 3 h for the first time. Nearly, monodisperse ~7 nm indium tin oxide (ITO) nanocrystals without any agglomeration were efficiently synthesized by pyrolysis of the as-synthesized precursors without using additional organic solvents under different conditions. It was found that both pyrolysis temperature and Sn doping level significantly influenced the particle size and size distribution of the ITO nanocrystals. A lower pyrolysis temperature and a higher Sn doping level resulted in a smaller particle size of the ITO nanocrystals. Addition of 1-octadecene solvent in the pyrolysis reaction could lead to a narrow particle size distribution of the ITO nanocrystals. In addition, all the as-synthesized ITO nanocrystals could be dispersed homogeneously in non-polar solvents such as *n*-hexane and chloroform without using surfactants forming optically clear solutions, which were used to prepare ITO/PVB nanocomposite film as interlayer for making laminated glass in solar control glazing.

S. Luo · D. Yang · J. Feng · K. M. Ng (✉)
Department of Chemical and Biomolecular Engineering, The Hong Kong University of Science and Technology, Clear Water Bay, Kowloon, Hong Kong
e-mail: kekmng@ust.hk

Keywords ITO nanocrystals · Precursor · Pyrolysis · Non-agglomerated · Solar control glazing

Introduction

Transparent conductive oxide (TCO) materials have received widespread attention owing to their high optical transparency, better electrical conductivity, and corresponding wide applications in devices such as touch panels, flat panel displays, solar cells, transparent electrode, and smart windows (Ginley et al. 2010). Tin-doped In_2O_3 (ITO), which is admirable candidate in most of these applications due to its highest available transmissivity for visible light combined with the lowest electrical resistivity within this class of TCO materials, shares more than 90 % transparent electrode market (Sunde et al. 2012). Normally, ITO thin films are fabricated via gas-phase deposition methods, such as *dc* and *rf* magnetron sputtering (Ginley et al. 2010). However, gas-phase deposition methods are inconvenient to form a thin film on flexible or heat sensitive substrates (e.g., plastics and paper). Moreover, the traditional gas-phase deposition methods are expensive and time consuming. In these regards, simple solution deposition pathway should be an attractive and promising alternative for film fabrication (Pasquarelli et al. 2011). With controlled size, morphology, and composition, well-dispersed TCO nanocrystals solution

can serve as inks for the inkjet printing or roll to roll production (Dattoll and Lu 2011).

In order to obtain high quality ITO nanocrystals, many methods have been designed and developed for the synthesis of the ITO nanocrystals such as co-precipitation (Li et al. 2006; Yu et al. 2004; Gao et al. 1999; Nam et al. 2001), electrolysis (Nakashima et al. 1995), sol–gel (Toki and Aizawa 1997; Jeon and Kang 2008), spray pyrolysis (Ogi et al. 2006; Jang et al. 2006; Itoh et al. 2004), solvothermal synthesis (Lee and Choi 2005; Endo et al. 2008; Sasaki et al. 2010), alloy oxidation (Peng et al. 2002; Yarema et al. 2012), emulsion technique (Sujatha Devi et al. 2002), and mixing followed by calcination (Yanagisawa and Udawatte 2000; Udawatte and Yanagisawa 2001). Among these, the solution-based synthetic routes are the most versatile. It is well known that the common co-precipitation method causes irregular and seriously agglomerated nanoparticles. Accordingly, there is a need to develop a better method for synthesizing ITO nanocrystals.

During the past 10 years, the thermolysis approach has been used to produce high quality metal oxide nanocrystals (Park et al. 2004, 2007; Lee et al. 2013), and the ITO nanocrystals with smaller particle size and narrow size distribution have been synthesized via the method (Bühler et al. 2007; Gilstrap et al. 2008; Choi et al. 2008; Sun et al. 2010; Lee et al. 2012). And furthermore, due to excellent dispersibility of ITO nanocrystals in the assigned solvent, they can serve as functional fillers in polymer matrix to produce polymer-based nanocomposite materials, which can improve the performance of the corresponding polymer (Liu et al. 2012). However, this method consumes a large amount of high boiling point organic solvents such as ODE. Another issue that should be considered is the cost and availability of the organo-metallic precursors. Hence, to develop an efficient method with a low cost for the synthesis of ITO nanocrystals with controlled particle size and size distribution has not only academic significance but also practical industrial applications.

Our group had developed an efficient and economical method in preparation of metal oxide particles. Metal oxide particles could be synthesized by pyrolyzing organo-metallic precursors, which are obtained by the reaction between metals and fatty acids at elevated temperatures (Yang et al. 2014). For example, nearly monodisperse In_2O_3 nanocrystals have been successfully prepared via the one-pot pyrolysis reaction (Luo et al. 2013). In this paper, we produce $\sim$7 nm ITO nanocrystals based on the precursor obtained by a direct reaction between metals (indium and tin) and molten stearic acid. The particle size of the nanocrystals can be controlled by tuning engineering factors such as pyrolysis temperature and tin doping level. When these ITO nanocrystals are dispersed in non-polar solvents such as chloroform, toluene, or *n*-hexane, optically clear solutions formed without any surfactants, which are stable for several months even a year without any precipitates. The application of the dispersed ITO nanocrystals in solution to prepare ITO/PVB nanocomposite films as interlayers for making laminated glass in solar control glazing is also conducted and discussed.

Experimental details

Chemicals

Raw indium metal (indium ingot, 99.995 %) and tin metal (tin granule, 99.999 %) were purchased from Zhuzhou Smelter Group Co., LTD, PRC; stearic acid (95 %), 1-octadecene (ODE, 90 %), and polyvinyl butyral (PVB) resin were obtained from Sigma-Aldrich Company; chloroform (99.8 %) and ethanol (99.9 %) were from Merck, and toluene (99.7 %) and *n*-hexane (95 %) were from Mallinckrodt. All the chemicals were used as received without any further purification.

Synthesis of indium–tin stearate precursors

0.01 mol of indium metal (1.15 g), 0.001 mol of tin granule (0.12 g, the amount of tin depends on the Sn doping level), and 0.034 mol of stearic acid (10.18 g) were introduced into a 50 mL condenser-equipped three-neck round-bottom flask. Then, the raw materials in the flask were heated from room temperature to 260 °C, and kept at that temperature with vigorous stirring for 3 h under a continuous nitrogen flow. (The function of the nitrogen atmosphere is to prevent the stearic acid from oxidation in air.) After 3 h, two metals disappeared, indicating that both of them reacted with stearic acid completely, and formed an optically clear solution with light yellow color. Consequently, the indium–tin stearate precursor in

waxy solid form was obtained by cooling the solution to the room temperature, which was used for characterization of the precursor.

Synthesis of ITO nanocrystals by pyrolysis without using any additional organic solvents

The solid indium–tin stearate precursor in the flask was heated from room temperature to 300 °C with a heating rate of 10 °C/min and was held at 300 °C for 3 h for the pyrolysis reaction under a nitrogen atmosphere. After 3 h, the flask was cooled down to the room temperature, and a blue precipitate at the bottom of the flask was observed. Then, the precipitate was washed by hot ethanol to remove the by-products, and dried at 80 °C overnight under vacuum. Finally, the ITO nanocrystals in powder form were obtained. It should be stressed that in our pyrolysis reaction, the precursor itself plays the role of a solvent and no additional high boiling point organic solvents such as ODE was used, which is significantly different from the reactions for the synthesis of nanocrystals reported before (Park et al. 2004, 2007; Lee et al. 2013; Bühler et al. 2007; Gilstrap et al. 2008; Choi et al. 2008; Sun et al. 2010; Lee et al. 2012).

Laminated glass with solar control glazing using ITO/PVB nanocomposite film as interlayer

In order to prepare laminated glass in solar control glazing, transparent ITO/PVB nanocomposite films with different ITO concentrations in PVB matrix were prepared. 1.0 g PVB and certain amount of 25 mg/mL ITO chloroform solution were added into 10 mL chloroform and vigorously stirred to obtain optically clear ITO/PVB solution. Then, 1 mL of the prepared solution was poured into a PP mold (20 mm × 30 mm × 15 mm). After that, the mold was transferred to a fume hood to evaporate the solvent overnight. After the solvent evaporated completely, a transparent ITO/PVB nanocomposite film was obtained. The thickness of the film was measured by a digital caliper. Three concentrations of ITO in PVB matrix were used, which are 0.2, 1.0, and 2.0 wt %, respectively. The ITO/PVB nanocomposite film was carefully intercalated to two pieces of commercial glass (20 mm × 20 mm, and 3 mm in thickness). Finally, the laminated glass using the ITO/PVB nanocomposite film as an interlayer was prepared at 140 °C for 1.5 h under compression, followed by cooling down to the room temperature.

Characterization

Thermo gravimetrical analysis (TGA) of the indium–tin stearate precursor was performed on a TGA (Perkin Elmer, UNIX/TGA7) from room temperature to 700 °C in a nitrogen atmosphere with a heating rate of 10 °C/min. Fourier transform infrared spectra (FT-IR) of the indium–tin stearate precursor were obtained by using an FT-IR spectrometer (Bio-Rad, FTS6000) with attenuated total reflection (ATR) mode. Phase identification and structural analysis of the ITO nanocrystals were conducted on a Phillips X'pert Pro X-ray diffractometer equipped with Cu Kα radiation ($\lambda = 1.54056$ Å) at a scan rate of 0.5°/s and 2θ from 10° to 70°, operating at 40 kV and 40 mA. Electron micrographs of the ITO nanocrystals were taken using a transmission electron microscope (TEM) (JEOL-2100) with an accelerating voltage of 200 kV, equipped with a Bruker energy-dispersive X-ray spectroscope (EDXS) and selected-area electron diffraction (SAED). The TEM samples were prepared by dropping an *n*-hexane dispersion of the ITO nanocrystals onto a copper grid coated with an amorphous carbon layer, followed by drying in a vacuum desiccator. UV–Vis-NR spectra of the laminated glass using the ITO/PVB nanocomposite film as the interlayer were recorded by UV–Vis spectrometer (Perkin Elmer, Lambda20) and FT-NIR spectrometer (Bruker, Vertex70), respectively.

Results and discussion

Synthesis and identification of indium–tin stearate precursor by a direct reaction between metals and molten stearic acid

Indium and tin were used to react with stearic acid in a flask at 260 °C under a nitrogen atmosphere. It was observed that some bubbles continuously came out from the reaction solution, which were identified to be hydrogen and gave a clear typical signal indicating that a reaction between metals and acid occurred indeed. After reaction, the solid product was characterized by FT-IR spectroscopy (ATR). Figure 1 displays the FTIR spectra of the solid product as well as a

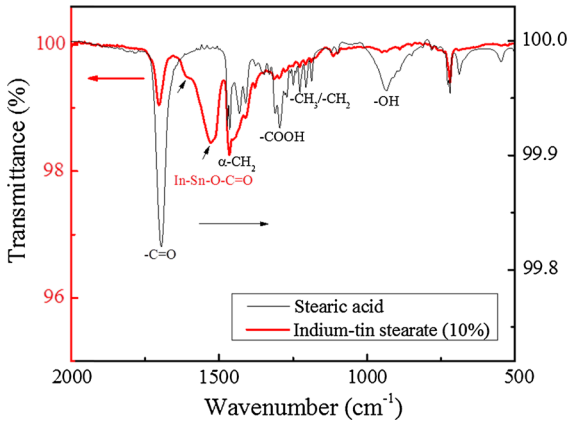

Fig. 1 FT-IR spectra of the stearic acid (*black*) and indium–tin stearate (*red*). The assignments of the main IR vibration bands of the spectrum are also showed. (Color figure online)

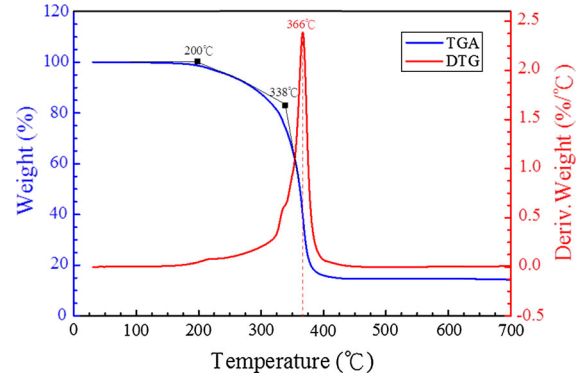

Fig. 2 TGA and DTG curves of indium–tin stearate. The displayed temperatures 200 and 338 °C are the estimated nucleation and main growth temperature, respectively

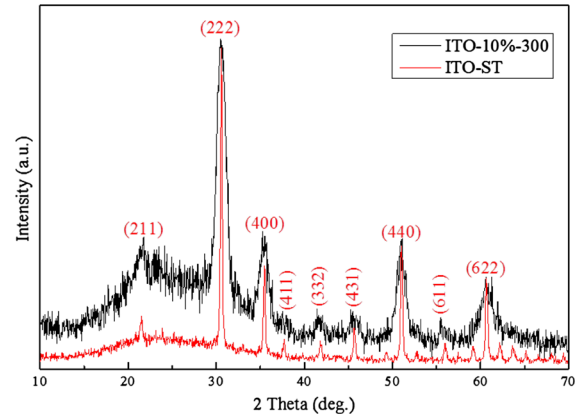

Fig. 3 XRD patterns of ITO samples. The standard pattern of *bcc* In_2O_3 was indexed (JCPDS #06-0416)

stearic acid sample for comparison. The assignments of the main IR vibration bands of the spectrum are also presented in Fig. 1. The spectrum of the product shows two asymmetric COO^- stretching peaks (1,610 cm^{-1} and 1,531 cm^{-1}) of metal carboxylate groups from 1,510 to 1,630 cm^{-1} which are the characteristic peaks different from the spectrum of the stearic acid (Gilstrap et al. 2008). Moreover, the dramatically weakening of –OH(δ) stretching peak at 943 cm^{-1} and –COOH(δ) stretching peak at 1,294 cm^{-1} also indicates that the stearic acid reacted with the metals, resulting in the formation of indium–tin carboxylate.

Synthesis of ITO nanocrystals via pyrolysis without using any additional organic solvents

Pyrolysis of organo-metallic precursors at high temperature is one of the most versatile routes in producing ITO nanocrystals with controllable size and shape, and the thermal stability of the organo-metallic precursors under synthetic conditions is also of great importance in nuclei generation and nanocrystals growth (Park et al. 2004). In this study, TGA was employed to investigate the pyrolysis behavior of the indium–tin stearate precursor under a nitrogen atmosphere. Figure 2 depicts the TGA curve of the precursor revealing that the pyrolysis mainly occurred at about 280–350 °C. When the temperature reached 450 °C, the weight loss stayed unchanged, illustrating that the precursor had decomposed completely to generate ITO product.

The pyrolysis of the indium–tin stearate precursor was conducted at 300 °C under a nitrogen atmosphere for 3 h. The blue product was obtained in powder form and named as ITO-10 %-300. The structure and phase purity of the final product were studied by powder X-ray diffraction (XRD) technique. The XRD pattern of ITO-10 %-300 is displayed in Fig. 3. The broad peaks centered at the peak positions match quite well with the main diffraction peaks of the body-centered cubic indium oxide (JCPDS file No. 06-0416), and no peaks of discernable tin oxide or other indium oxide compounds were detected. The XRD pattern clearly confirms that indium ion was replaced by the tin ion in the lattice. As a result, the ITO nanocrystals consist of a solid solution of the indium tin oxide.

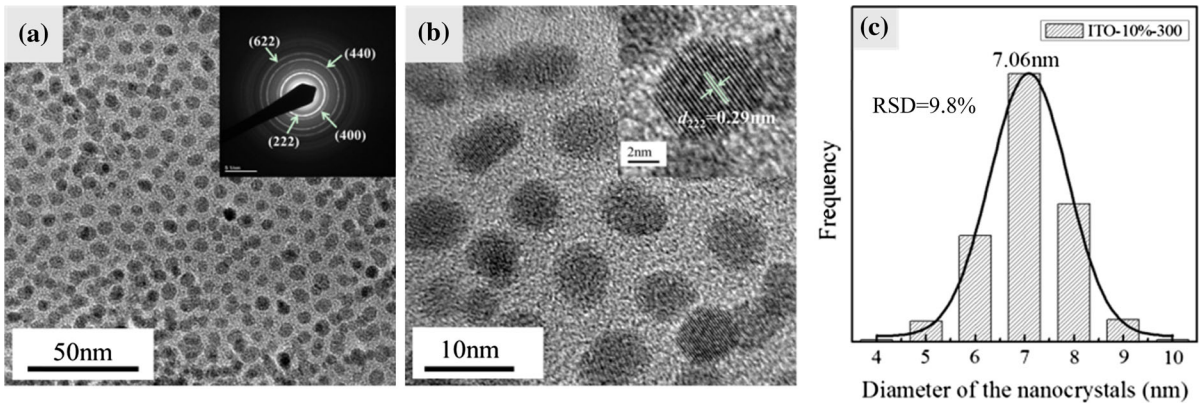

Fig. 4 **a** Low resolution and **b** high resolution TEM images of the ITO-10 %-300 nanocrystals. The SAED pattern is shown as an *inset* in (**a**). **c** The relative size distribution histogram. The curve is the corresponding Gaussian fit

The average crystallite size was calculated from the XRD patterns using the Debye–Scherrer equation below:

$$D = \frac{k\lambda}{\beta cos\theta} \quad (1)$$

where D is the crystallite size in nanometers, λ is the wavelength of X-ray in nanometers (Cu Kα = 0.154 nm), β is the calibrated full width at half maximum (FWHM) of the XRD in radian, θ is the Bragg diffraction angle, and $k = 0.89$ for most common case. Base on the Eq. 1, the calculated average crystallite diameter of the ITO product is 7.45 nm according to the FWHM of the four most intense peak reflections [(222), (400), (440), and (622)] after instrument correction (Caruntu et al. 2010).

The morphology of the ITO nanocrystals was also examined by TEM. Figure 4a shows the TEM image of ITO-10 %-300, which exhibits several characteristics. The ITO nanocrystals exist in particle form without agglomeration, and are also in nearly monodisperse state which is caused by the presence of surfactant-like chemicals on the surface of the ITO nanocrystals. The selected-area electron diffraction (SAED) pattern of the ITO nanocrystals can be attributed to the (222), (400), (440), and (622) diffraction planes, which are supported by the XRD characterization. As shown in Fig. 4b, the high resolution TEM image reveals that the nanoparticle has a single crystalline nature with an atomic lattice fringe image of 0.29 nm corresponding to interplanar spacing of (222) lattice plane. Measurement of 300 random particles of ITO-10 %-300 sample in the TEM image indicates that the ITO nanocrystals have an average diameter of 7.06 nm with a narrow size distribution and the corresponding RSD (relative standard deviation) was 9.8 %, which agrees well with the result calculated from the equation, as displayed in Fig. 4c. In addition, the data also demonstrate that each particle only contains one domain without any internal grain boundaries, declaring the homogenous doping on the lattice level. The XPS result indicated that the molar ratio of tin to indium is 10.2 % in the as-synthesized ITO nanocrystals, which is consistent with the initial Sn/In ratio.

It should be noticed that our pyrolysis reaction was conducted without using any additional organic solvents such as ODE, which is different from the typical pyrolysis reaction using ODE as reported by the literature (Park et al. 2007; Lee et al. 2013). Thus, our pyrolysis reaction without any additional solvents can lead to an efficient and simple way to synthesize ITO nanocrystals, because in the pyrolysis reaction the concentration of the indium–tin precursor is much higher than that in the reported literature (Bühler et al. 2007; Gilstrap et al. 2008; Choi et al. 2008; Sun et al. 2010; Lee et al. 2012).

The produced nearly monodisperse ITO nanocrystals can be dispersed in non-polar solvents such as chloroform, toluene, or *n*-hexane and form an optically clear solution. The 10 wt % ITO solution displayed a complete lack of agglomeration and could be stable for a few months even a year. This unique

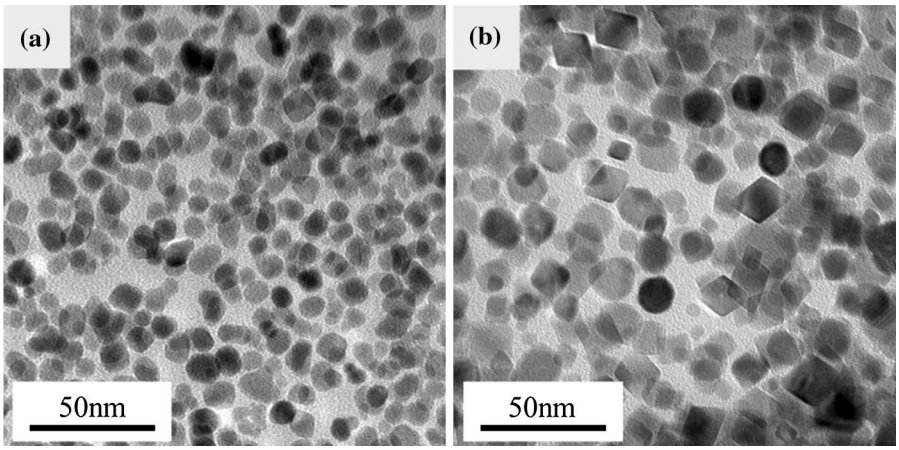

Fig. 5 TEM images of the obtained ITO products at different pyrolysis temperatures. **a** ITO-10 %-320 and **b** ITO-10 %-350

property of the ITO nanocrystals also builds up a solid foundation for the preparation of transparent ITO/polymer nanocomposite film because many typical transparent polymers such as PVB, PMMA, and PC can be easily dissolved in typical non-polar solvents such as chloroform. Accordingly, using a conventional solution casting method, transparent ITO/polymer nanocomposite films can be obtained for various industrial applications.

Effect of pyrolysis temperature

It is well accepted that pyrolysis temperature is a key factor in the synthesis of ITO nanocrystals. Many researchers have studied the effect of pyrolysis temperature on the particle size of the nanocrystals (Park et al. 2004, 2007; Lee et al. 2013). The pyrolysis temperatures investigated are determined to be at 280, 300, 320, and 350 °C.

When the pyrolysis reaction of the indium–tin stearate precursor was conducted at 280 °C for 3 h, it was observed that no obvious ITO nanocrystals were precipitated, indicating that the pyrolysis reaction of the precursor at this temperature was slow. When the pyrolysis reaction of the precursor was carried out at 300 °C for 3 h, the obtained results are presented in "Synthesis of ITO nanocrystals …" section already. When the pyrolysis reaction took place at 320 °C, the average particle size of the ITO nanocrystals is determined to be about ~12 nm by TEM as shown in Fig. 5a, illustrating that particle size of the ITO nanocrystal increases from about 7 to 12 nm when the pyrolysis temperature increases from 300 to 320 °C, the tendency in total agreement with the previously published results (Lee et al. 2013; Jin et al. 2013). Figure 5a also depicts that some ITO nanocrystals are present with a nearly octahedron morphology, suggesting the formation of ITO nanocrystals with two different morphologies at that temperature. When the pyrolysis temperature was further increased to 350 °C, explosive pyrolysis reaction occurred and completed rapidly, it was found that there are more octahedral ITO nanocrystals formed in the product, as displayed in Fig. 5b. Thus, the pyrolysis temperature window for the production of more uniform ITO nanocrystals ranges from 300 to 320 °C.

Effect of addition of ODE solvent

In the early studies on the synthesis of metal oxide nanocrystals by pyrolysis, many researchers used the high boiling point solvents such as 1-hexadecene (b.p. 274 °C), 1-octadecene (ODE, b.p. 317 °C), and trioctylamine (TOA, b.p. 365 °C) during the pyrolysis reaction. Their results clearly indicate that as the boiling point of the solvents increases, the precursor in the solvent shows a higher reactivity, resulting in an increase in the particle size of the ITO nanocrystals (Park et al. 2004; Ye et al. 2010). In order to investigate the effect of addition of ODE solvent in the pyrolysis reaction of indium–tin stearate precursor, a parallel pyrolysis experiment using ODE as solvent was carried out at 300 °C for 3 h, and the concentration of the indium and tin ions was 0.15 M. Blue ITO

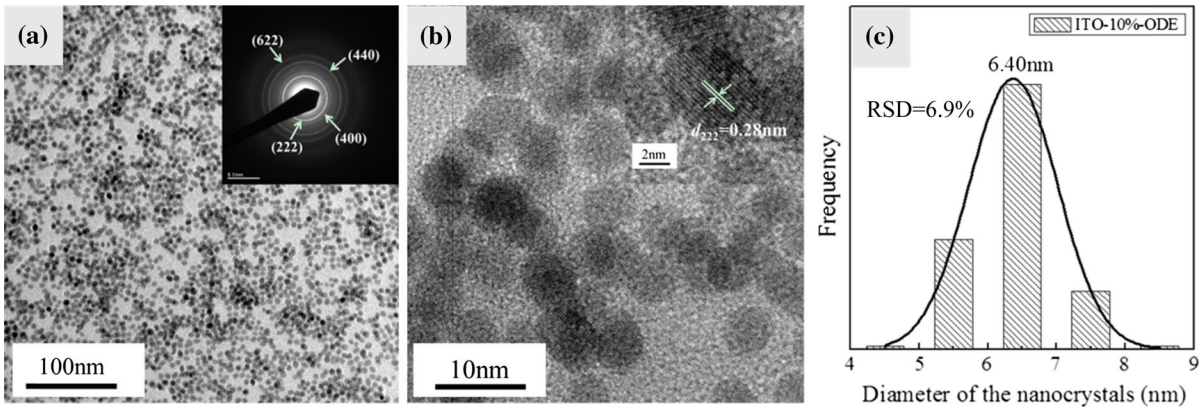

Fig. 6 **a** Low resolution and **b** high resolution TEM images of the ITO-10 %-ODE nanocrystals. The SAED pattern is shown as an *inset* in (**a**). **c** The relative size distribution histogram. The curve is the corresponding Gaussian fit

nanocrystals in powder form were obtained after purification and labeled as ITO-10 %-ODE.

Figure 6 presents the TEM image of the ITO-10 %-ODE sample, displaying the as-synthesized ITO nanocrystals with an average particle size of 6.40 nm corresponding a RSD of 6.9 %. When compared with the results shown in "Synthesis of ITO nanocrystals …" section, it is observed that even though the ODE solvent has no significant effect on the nucleation process, the concentration of the nuclei in the reaction solution decreases, leading to a narrow particle size distribution. Moreover, the diameter of the nanocrystals has a slight decline since the ODE could stop the nanocrystals from growing to some extent. The comparisons between Figs. 4 and 6 also illustrate that addition of ODE to the pyrolysis reaction does not impose any significant impact on the particle size of the ITO nanocrystals. From point view of an engineering aspect, our one-pot pyrolysis of simple raw materials and forthright procedure pave it ideal for industrial scale-up of the synthesis of the ITO nanocrystals.

Effect of different Sn doping levels

Indium tin oxide nanocrystals exhibit splendid opto-electronic performance that is quite different from that of its matrix crystal indium oxide, which is considered as a wide band gap transparent semiconductor. The optical and electronic properties are related to the energy level structures and valence state of the tin dopants (Sun et al. 2010; Jin et al. 2013). During the pyrolysis reaction, it is hard to control the homogeneity of the doped product because the organo-metallic precursors may have different decomposition temperatures (Ito et al. 2012). Normally, TGA profile is regarded as the most efficient way to depict the thermal behavior of the organic metal salt precursor. In general, congeneric/homologous metal salts show similar thermal attributes. Figure 7 illustrates that the synthesized indium–tin stearate precursors with different Sn doping levels had similar decomposition tendency, and no significant disparity among them was observed. Most importantly, the curves indicate that the sharp decline of weight loss mainly concentrated at about 300–375 °C, implying that the indium stearate and tin stearate most likely decomposed simultaneously, and tin ions would insert the indium oxide lattices homogenously rather than exist

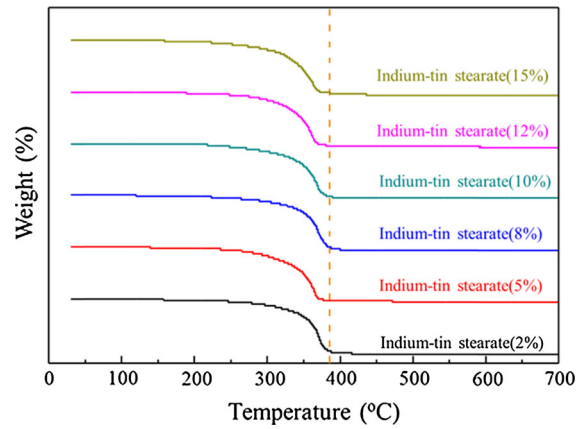

Fig. 7 TGA curves of the indium–tin stearate with different Sn doping levels

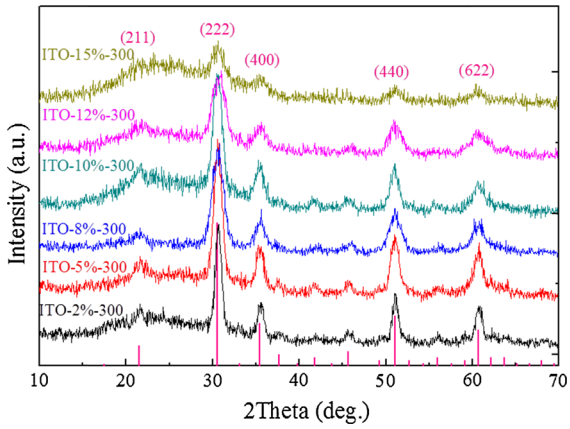

Fig. 8 XRD patterns of the ITO nanocrystals with different Sn doping levels. The *pink vertical lines* represent the standard pattern of *bcc* In_2O_3 (JCPDS #06-0416). (Color figure online)

as an individual phase until the amount of tin reaches the tolerated limit. Too high concentration of tin dopants in the indium oxide lattices will cause significant lattice distortion even separation from the host.

The XRD patterns of ITO-(2–15) %-300 are demonstrated in Fig. 8. Obviously, all the main peaks match well with the main diffraction peaks of *bcc* indium oxide (JCPDS file No. 06-0416), and the peaks become broader as the Sn dopant concentration increases, resulting in smaller particle size of the ITO nanocrystals. This is further confirmed by the TEM observations as shown in Fig. 9, indicating that as Sn doping levels increase from 2 to 15 wt %, the average particles size of the corresponding ITO nanocrystals decreases from 12 to 6.5 nm.

No other peaks of impurity were found even in the ITO-15 %-300 sample, which promised the distribution of tin ions in the indium oxide lattices. The well mixed indium–tin stearate precursor provides an efficient way to synthesize the ITO nanocrystals with a wide range of Sn doping levels, resulting in the products with a narrow size distribution. All the products could be dispersed in chloroform to form optically clear solutions as shown in Fig. 10, in which the concentration of the ITO in chloroform is 35 mg/mL. It was also observed that as the tin doping level increases, the color of the dispersion of ITO nanocrystals in chloroform becomes darker, indicating a blue shift in the absorption of the dispersion in visible light range (Lee et al. 2012).

Application of ITO nanocrystals in laminated glass in solar control glazing

It is well known that ITO nanocrystals display unique optical properties: high transmission in the visible light region, high reflection in the IR light region, and high absorbance in the UV light region (Yin et al. 2007). Their excellent optical properties make them to be used in the preparation of transparent polymer-based functional films for fabricating the laminated window glass in solar control glazing. Smith et al. (2002) reported that nanoparticle-doped PVB foils made by extrusion process can provide laminated windows and polymer glazing for good solar control with high visual and daylighting performance.

In this study, using conventional solution casting method, we successfully fabricated transparent ITO/PVB nanocomposite films with three different ITO concentrations in PVB matrix, which were used for making laminated glass. The inset in Fig. 11 shows a photo of a laminated glass using an ITO/PVB nanocrystal nanocomposite film with an ITO concentration of 1 wt % as an interlayer, displaying excellent transparency of the laminated glass. Figure 11 presents the UV–Vis spectra of the four laminated glass samples, which illustrate that in the range of visible light, all the four samples show over 80 % transmittance. Thus, addition of ITO nanocrystals in PVB matrix does not significantly influence the transmittance of the laminated glass samples. The high transmittance over 80 % of the laminated glass is even better than that of commercial laminated glass as reported in the literature (Smith et al. 2002). The physics behind this phenomenon is that the ITO nanocrystals can provide spectrally absorption without any scattering.

In order to evaluate the performance of the laminated glass in solar control glazing, the IR spectra of the four samples were measured, and are presented in Fig. 12. The spectra clearly show that addition of ITO nanocrystals to the PVB matrix can drastically impose a significant impact on the transmission of IR light in the range of 900–2,500 nm. In case of laminated glass sample using a neat PVB film as an interlayer, about 80 % IR light can pass through the laminated glass, indicating that the laminated glass does not show any significant effect in solar control glazing. However, when ITO/PVB nanocomposite films are used as interlayers for the laminated glass,

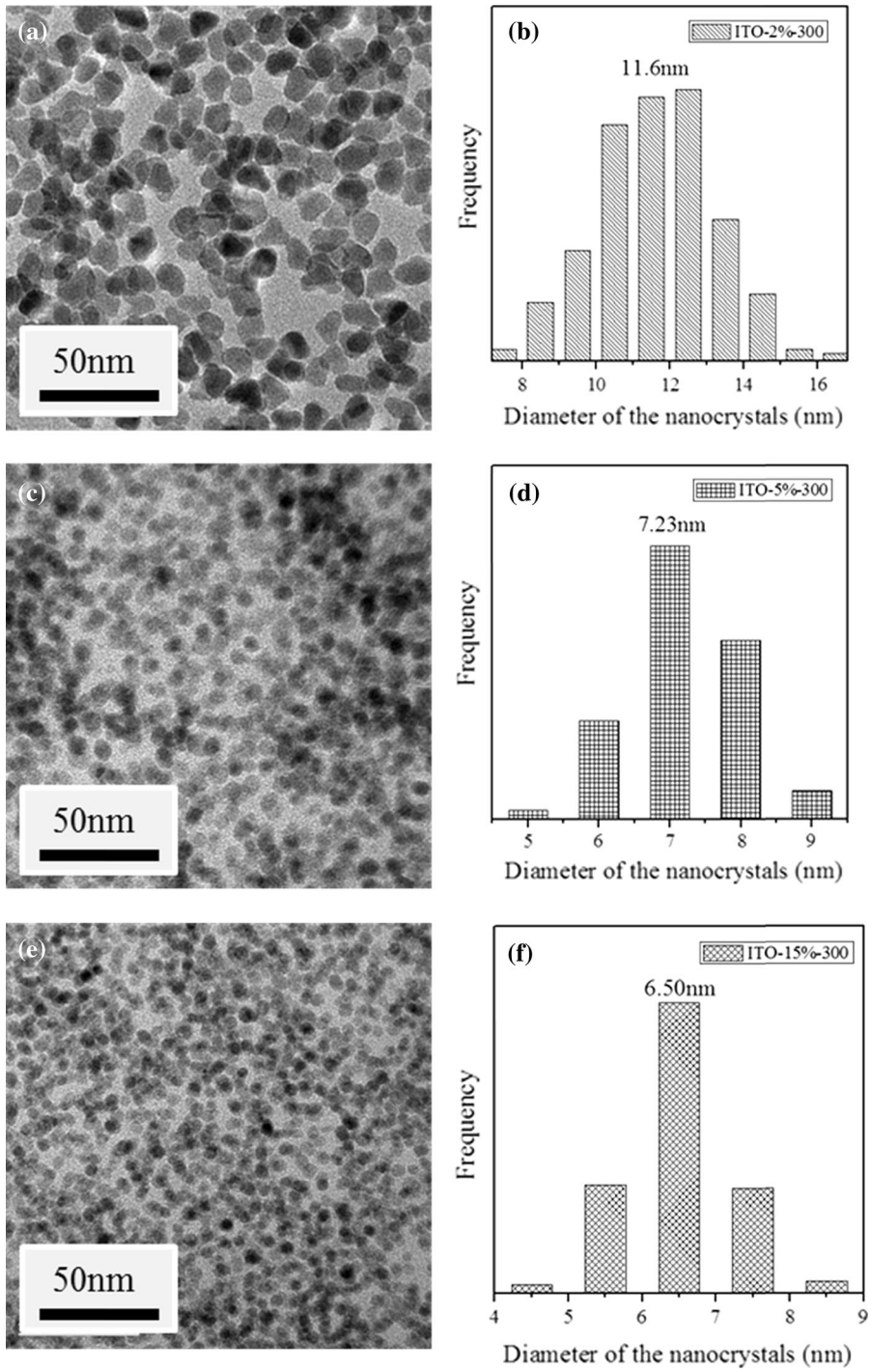

Fig. 9 TEM images and the relative size distribution histograms of the ITO nanocrystals with different Sn doping levels. **a**, **b** ITO-2 %-300, **c**, **d** ITO-5 %-300 and **e**, **f** ITO-15 %-300

the transmission of the IR light significantly decreases particularly when the ITO concentration in PVB matrix reaches 1 wt %. As the concentration of ITO nanocrystals in the PVB matrix increases from 0 to 0.2, 1.0, and 2.0 wt %, the transmission of the IR light for the four samples calculated is determined to be 81.3, 80.8, 44.3, and 42.5 %, respectively. When the ITO concentration is over 1 wt %, further increase in

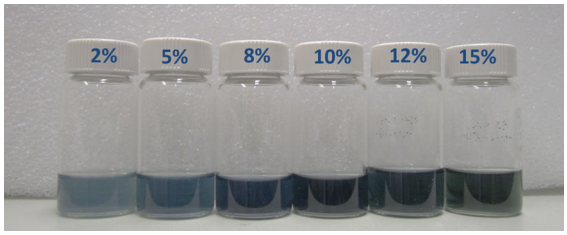

Fig. 10 A photo of various dispersions of ITO nanocrystals with different Sn doping levels in chloroform

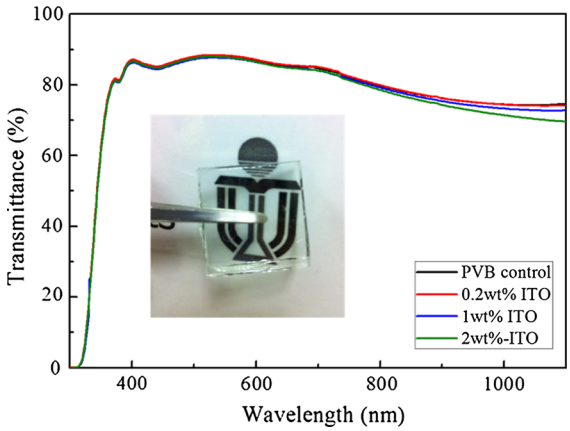

Fig. 11 UV–Vis spectra of laminated glass samples using different ITO/PVB nanocomposite films as an interlayer. The *inset* is a photo of a laminated glass with 1.0 wt % ITO in PVB matrix

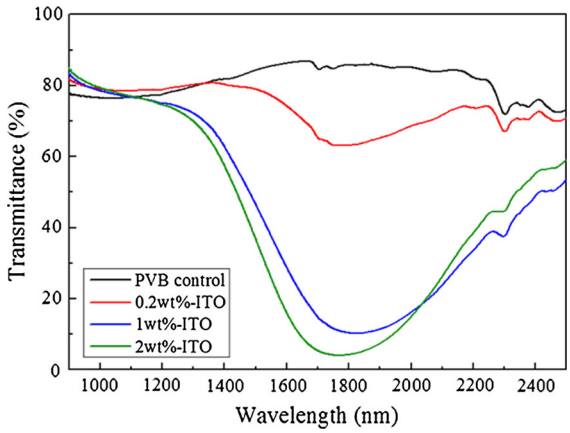

Fig. 12 IR spectra of laminated glass samples using different ITO/PVB nanocomposite films as an interlayer

concentration does not significantly reduce the transmission of the IR light at all. The low transmission of IR light in the wavelength range of 900–2,500 nm about 44.3 % for the laminated glass is comparable to that of commercial laminated glass as reported in the literature (Smith et al. 2002). The results also illustrate that the ITO nanocrystals obtained in this studies have a promising industrial applications to make laminated glass in solar control glazing.

Conclusions

In summary, we synthesized indium–tin stearate precursor by a direct reaction between metals (indium and tin) and molten stearic acid under a nitrogen atmosphere at 260 °C for 3 h for the first time, which built up a solid foundation for the scaling up of the synthesis of ITO nanocrystals in industry. Nearly, monodisperse ~7 nm ITO nanocrystals without any agglomeration were synthesized by direct pyrolysis of the as-synthesized precursors without using any additional organic solvents under different conditions, which provide an efficient approach to synthesize ITO nanocrystals. A lower pyrolysis temperature and a higher Sn doping level could result in a smaller particles size of the ITO nanocrystals. Addition of a small amount of ODE in pyrolysis reaction could lead to a narrow particle size distribution of the ITO nanocrystals. In addition, the as-synthesized ITO nanocrystals could be dispersed homogeneously in non-polar solvents such as *n*-hexane, toluene, and chloroform, forming optically clear solutions. The importance of the results is to open a window to prepare various transparent ITO/polymer nanocomposite films for different industrial applications such as ITO/PVB nanocomposite film as interlayer for making laminated glass in solar control glazing. The laminated glass using a ITO/PVB nanocomposite film as an interlayer with 1.0 wt % ITO shows over 80 % transmittance in visible light range and smaller than 45 % transmittance in IR range (900–2,500 nm).

Acknowledgments The authors gratefully acknowledge the financial support from the University Grants Council of the Hong Kong Government. Also, the technical support of the Raith-HKUST Nanotechnology Laboratory (project no. SEG_HKUST08) at MCPF of HKUST is appreciated.

References

Bühler G, Thölmann D, Feldmann C (2007) One-pot synthesis of highly conductive indium tin oxide nanocrystals. Adv Mater 19:2224–2247

Caruntu D, Yao K, Zhang Z, Austin T, Zhou W, O'Connor CJ (2010) One-step synthesis of nearly monodisperse, variable-shaped In_2O_3 nanocrystals in long chain alcohol solutions. J Phys Chem C 114:4875–4886

Choi SI, Nam KM, Park BK, Seo WS, Park JT (2008) Preparation and optical properties of colloidal, monodisperse, and highly crystalline ITO nanoparticles. Chem Mater 20:2609–2611

Dattoll EN, Lu W (2011) ITO nanowires and nanoparticles for transparent film. MRS Bull 36:782–788

Endo Y, Sasaki T, Kanie K, Muramatsu A (2008) Direct preparation and size control of highly crystalline cubic ITO nanoparticles in a concentrated solution system. Chem Lett 37:1278–1279

Gao Z, Gao Y, Li Y, Li Y (1999) Effects of heat treatment on the microstructure of nanophase indium-tin oxide. Nanostruct Mater 11:611–616

Gilstrap RA, Capozzi CJ, Carson CG, Gerhardt RA, Summers CJ (2008) Synthesis of a nonagglomerated indium tin oxide nanoparticle dispersion. Adv Mater 20:4163–4166

Ginley DS, Hosono H, Paine DC (2010) Handbook of transparent conductors. Springer, New York, pp 1–25

Ito D, Masuko K, Weintraub BA, Mckenzie LC, Hutchison JE (2012) Convenient preparation of ITO nanoparticles inks for transparent conductive thin films. J Nanopart Res 14:1274

Itoh Y, Abdullah M, Okuyama K (2004) Direct preparation of nonagglomerated indium tin oxide nanoparticles using various spray pyrolysis methods. J Mater Res 19:1077–1086

Jang HD, Seong CM, Chang HK, Kim HC (2006) Synthesis and characterization of indium-tin oxide (ITO) nanoparticles. Curr Appl Phys 6:1044–1047

Jeon MK, Kang M (2008) Synthesis and characterization of indium-tin-oxide particles prepared using sol–gel and solvothermal methods and their conductivities after fixation on polyethyleneterephthalate films. Mater Lett 62:676–682

Jin Y, Yi Q, Ren Y, Wang X, Ye Z (2013) Molecular mechanism of monodisperse colloidal tin-doped indium oxide nanocrystals by a hot-injection approach. Nanoscale Res Lett 8:153

Lee JS, Choi SC (2005) Solvent effect on synthesis of indium tin oxide nano-powders by a solvothermal process. J Eur Cream Soc 25:3307–3314

Lee J, Lee S, Li G, Petruska MA, Paine DC, Sun S (2012) A facile solution-phase approach to transparent and conducting ITO nanocrystal assemblies. J Am Chem Soc 134:13410–13414

Lee J, Zhang S, Sun S (2013) High-temperature solution-phase syntheses of metal-oxide nanocrystals. Chem Mater 25:1293–1304

Li S, Qiao X, Chen J, Wang H, Jia F, Qiu X (2006) Effects of temperature on indium tin oxide particles synthesized by co-precipitation. J Cryst Growth 289:151–156

Liu H, Zeng X, Kong X, Bian S, Chen J (2012) A simple two-step method to fabricate highly transparent ITO/polymer nanocomposite films. Appl Surf Sci 258:8564–8569

Luo S, Yang D, Zhuang J, Ng KM (2013) Synthesis and characterization of nearly monodisperse deltoidal icositetrahedral In_2O_3 nanocrystals via one-pot pyrolysis reaction. CrystEngComm 15:8065–8068

Nakashima K, Saito T, Maekawa T (1995) Process for preparation of indium oxide-tin oxide powder. U.S. Patent: 5417816

Nam JG, Choi H, Kim SH, Song KH, Park SC (2001) Synthesis and sintering properties of nanosized In_2O_3-10wt% SnO_2 powders. Scripta Mater 44:2047–2050

Ogi T, Iskandar F, Itoh Y, Okuyama K (2006) Characterization of dip-coated ITO films derived from nanoparticles synthesized by low-pressure spray pyrolysis. J Nanopart Res 8:343–350

Park J, An K, Hwang Y, Park JG, Noh HJ, Kim JY, Park JH, Hwang NM, Hyeon T (2004) Ultra-large-scale syntheses of monodisperse nanocrystals. Nat Mater 3:891–895

Park J, Joo J, Kwon SG, Jang Y, Hyeon T (2007) Synthesis of monodisperse spherical nanocrystals. Angew Chem Int Ed 46:4630–4660

Pasquarelli RM, Ginleyb DS, Hayrea RO (2011) Solution processing of transparent conductors: from flask to film. Chem Soc Rev 40:5406–5441

Peng XS, Meng GW, Wang XF, Wang YW, Zhang J, Liu X, Zhang LD (2002) Synthesis of oxygen-deficient indium-tin-oxide (ITO) nanofibers. Chem Mater 14:4490–4493

Sasaki T, Endo Y, Nakaya M, Kanie K, Nagatomi A, Tanoue K, Nakamura R, Muramatsu A (2010) One-step solvothermal synthesis of cubic-shaped ITO nanoparticles precisely controlled in size and shape and their electrical resistivity. J Mater Chem 20:8153–8157

Smith GB, Deller CA, Swift PD, Gentle A, Garrett PD, Fisher WK (2002) Nanoparticle-doped polymer foils for use in solar control glazing. J Nanopart Res 4:157–165

Sujatha Devi P, Chatterjee M, Ganguli D (2002) Indium tin oxide nano-particles through an emulsion technique. Mater Lett 55:205–210

Sun Z, He J, Kumbhar A, Fang J (2010) Nonaqueous synthesis and photoluminescence of ITO nanoparticles. Langmuir 26:424–450

Sunde TOL, Garskaite E, Otter B, Fossheim HE, Sæterli R, Holmestad R, Einarsrud MA, Grande T (2012) Transparent and conducting ITO thin films by spin coating of an aqueous precursor solution. J Mater Chem 22:15740–15749

Toki M, Aizawa M (1997) Sol-gel formation of ITO thin film from a sol including ITO powder. J Sol-Gel Sci Technol 8:717–720

Udawatte CP, Yanagisawa K (2001) Fabrication of low-porosity indium tin oxide ceramics in air from hydrothermally prepared powder. J Am Ceram Soc 84:251–253

Yanagisawa K, Udawatte CP (2000) Preparation and characterization of fine indium tin oxide powder by a hydrothermal treatment and postannealing method. J Mater Res 15:1404–1408

Yang D, Ng KM, Chan SY (2014) Methods of metal oxide nanocrystals preparation. U. S. non-provisional Patent application

Yarema M et al (2012) From highly monodisperse indium and indium tin colloidal nanocrystals to self-assembled indium tin oxide nanoelectrodes. ACS Nano 6:4113–4121

Ye E, Zhang SY, Lim SH, Liu S, Han MY (2010) Morphological tuning, self-assembly and optical properties of indium oxide nanocrystals. Phys Chem Chem Phys 12:11923–11929

Yin Y, Zhou S, Gu G, Wu L (2007) Preparation and properties of UV-curable polymer/nanosized indium-doped tin oxide (ITO) nanocomposite coatings. J Mater Sci 42:5959–5963

Yu D, Wang D, Yu W, Qian Y (2004) Synthesis of ITO nanowires and nanorods with corundum structure by a co-precipitation-anneal method. Mater Lett 58:84–87